QUANTIFICATION OF SOLUBLE SOLIDS AND INDIVIDUAL SUGARS IN APPLES BY RAMAN SPECTROSCOPY: A FEASIBILITY STUDY

Olga Monago-Maraña[1,2], Nils Kristian Afseth[2], Svein Halvor Knutsen[2], Sileshi Gizachew Wubshet[2], Jens Petter Wold[2]

[1]Department of Analytical Sciences, Faculty of Science, Avda. Esparta s/n, Crta. de Las Rozas-Madrid, 28232, Las Rozas, Madrid, National Distance Education University (UNED), Spain

[2]Nofima AS – Norwegian Institute of Food, Fisheries and Aquaculture Research, Muninbakken 9-13, Breivika, Postboks 6122 Langnes, NO-9291 Tromsø, Norway

*corresponding author: olgamonago@ccia.uned.es; +34675673233

Abstract

This study reports the feasibility of using Raman spectroscopy for quantification of soluble solids and individual sugars in apple. Six different commercial apple varieties were measured by Raman spectroscopy at three different steps: 1) Intact apples with skin, 2) apples without skin and 3) juices obtained from apples. Results indicated that it is possible to measure Raman signals to a depth of 8 mm into the apple with a wide area Raman probe. Multivariate calibration models were established to evaluate how well Raman spectra can be used to estimate the quality parameters SSC (%), total sugars, glucose, fructose and sucrose. Estimation accuracy for SSC was comparable with what is achievable with near-infrared spectroscopy: Root mean square error of cross-validation (RMSECV) = 0.66, 0.46 and 0.72 % and coefficients of determination (R^2) = 0.70, 0.85 and 0.63 for intact apples, apples without skin and juices, respectively. Sucrose and glucose were well estimated with RMSECV of 2.8, 1.9, 2.1 mg/mL for glucose and 5.8, 3.9 and 3.7 mg/mL for sucrose, for the three sample cases, respectively. Coefficient of determination was higher than 0.82 for all models. Regression coefficients for all calibration models highlighted identifiable Raman bands that could be related to the target sugars.

Keywords: Raman spectroscopy; SSC; apples; non-destructive prediction; chemometrics; sugars.

1. Introduction

Apple is a widely produced and consumed fruit around the world. It is rich in sugar, vitamins, flavonoids, minerals and other nutrients attributed to health benefits. Sweetness is one of the most important components of fruit quality that determines the overall acceptability of apples (Harker et al., 2003; Janick et al., 1996). Sweetness is correlated to soluble solids content (SSC), which includes total solutes; e.g.; organic acids, amino acids, soluble pectins and has a major contribution from the sugars fructose, glucose and sucrose (Guan et al., 2015). SSC is an important parameter to determine flavour, ripeness as well as to predict optimal harvest time for apples. Refractometry of fruit juice is the standard method for SSC measurement, given as % or ^{o}Brix, unfortunately a destructive and rather time-consuming procedure. Quantification of individual sugars (fructose, glucose and sucrose) in apples are also of interest in connection with phenotyping and breeding programs, as well as for studying carbohydrate metabolism during ripeness and postharvest storage (Guan et al., 2015). For industrial purposes, breeding and research there is a strong need for rapid and non-destructive determination of SSC as well as the individual sugars in apples.

Near-infrared spectroscopy (NIRS) is already established as an efficient method for determination of SSC in apples. The method relies on absorption overtones and combination of vibrational bands mainly associated with -CH and -OH functional groups present in the different carbohydrates such as glucose, sucrose and fructose (López et al., 2016). Nicolaï et al., 2007 reviewed the status of non-destructive measurement of fruit quality by means of NIRS, and several studies show that a typical prediction error (root mean square error of prediction, RMSEP) for SSC is around 0.5 %. But this accuracy is usually obtained for individual apple varieties from the same season and from the same orchard. When calibrations are validated with apples from different seasons or origins, the RMSEP usually increases to 1-1.5 %. Nicolaï et al., 2007 concluded that to obtain a robust calibration model, the calibration data set should be rich in variation and include apples from different orchards and seasons. They regarded model robustness as the single most important concern in NIRS of horticultural produce. The use of NIRS for determination of individual sugars

in intact apples was newly reported by Lan et al. (2020). They collected spectra in the region 900-2500 nm from 840 apples of three varieties. Calibration models for fructose, glucose and sucrose were obtained with promising results (RMSEP = 1.9, 9.2 and 7.6 g/kg, respectively). The models were complex and no interpretation of the spectral data was offered (Lan et al., 2020).

Today, grading lines equipped with NIR sensors are commercially available (Nicolaï et al., 2007) and novel compact sensors have the potential to be used effectively in field and during storage. But the workload of proper calibration and continuous calibration maintenance is a considerable cost. It is therefore of interest to explore potential alternative non-destructive techniques. Raman spectroscopy is one such technique that is now available in more affordable and compact instrumentation. Raman spectra are in general more selective compared to NIR spectra, providing more narrow spectral bands with abundant and well resolved chemical information which is easier to interpret. It is well known that Raman spectroscopy is well suited for analysis and quantification of sugars in complex samples. Özbalci et al., 2013 showed that fructose, glucose, maltose and sucrose in water solutions can be clearly discriminated, and also quantified in diluted honey samples by Raman spectroscopy using a laser excitation of 785 nm. Calibration models based on PLS regression gave correlation coefficients higher than 0.95 for all the individual sugars (Özbalci et al., 2013). Individual sugars in soft drinks have also been quantified with Raman, using external calibration curves with sugar standards (Ilaslan et al., 2015). In this case, Raman spectroscopy performed equally well as high performance liquid chromatography. Raman spectroscopy is suitable for process monitoring in liquid systems and has been used for real time quantification of total sugars with high accuracy (R^2 = 0.99, RMSECV = 0.17 g/L) during wine fermentation (Wang et al., 2014). Total sugars were also determined in wine samples by FT-Raman (RMSEP = 0.85 g/L) and better results were obtained compared to mid IR (RMSEP = 1.2 g/L) and NIRS (RMSEP = 1.4 g/L). Raman spectroscopy has also been used for adulteration detection of coconut water with different types of sugars and was demonstrated to detect very low levels of added single sugars, i.e. 2.1 %, 2.6 % and 1.9 % for glucose, fructose and sucrose, respectively (Richardson et al., 2019).

One important technical aspect when considering Raman spectroscopy for analysis of intact solid food matrices is representative sampling. Novel Raman system designs, such as spatially offset Raman spectroscopy (SORS) and wide area Raman spectroscopy, allow deeper optical sampling in biological tissues (Esmonde-White et al., 2017; Monago-Maraña et al., 2021). This makes them highly relevant for measuring internal quality in foods (Afseth et al., 2014). An example is the use of SORS for evaluation of internal maturity of tomatoes (Qin et al., 2012). As far as we know, there are no reported studies on the determination of SSC or individual sugars in intact apples by Raman spectroscopy. Hence, the aim of this study was to elucidate the potential for such an application. Raman measurements employing a wide area Raman probe were performed on a total of 60 apples of six different varieties at three steps: 1. intact apples, 2. apples without skin, and 3. on the juice from the apples. From these measurements, regression models for SSC (%), total sugars and contents of sucrose, glucose and fructose were obtained. In addition, the optical sampling depth in apples was investigated.

2. Materials and methods

2.1. Samples and chemicals

A total of 60 samples were used in this study. Ten apples of six different varieties were selected from the Norwegian grocery market in 2020: Granny Smith (variety 1), Royal Gala Kanzi (variety 2), Royal Gala (variety 3), Golden Delicious (variety 4), Pink Lady (variety 5) and Ecology Red apples (variety 6). All samples were purchased May 2020 and could thus be expected to be fully ripened. They were kept at 4 ºC until further analysis.

Glucose, fructose and sucrose standards were purchased from Merck (Oslo, Norway). Trehalose was obtained from VWR Life Science (Oslo, Norway). Sodium acetate and sodium hydroxide solution (50 – 52 % in water), used for the mobile phases, were bought from Merck (Oslo, Norway). Milli-Q water was obtained from a Milli-Q water system (Merck, Oslo, Norway).

2.2. Reference analysis

Soluble solids content (SSC), expressed in %, was determined at 25 ºC with a RE40 digital refractometer (Mettler Toledo AS, Oslo) on the fresh juice samples obtained, from peeled apples after removing the peduncle, with a juice maker. Juices were then frozen for further analysis of glucose, fructose and sucrose. Individual sugars were determined following the method described by Helgerud et al., 2016. An aliquot of juice was diluted (1:2000) with Milli-Q water and containing 10 μg/mL of trehalose as internal standard in each sample. A High-Performance Anion Exchange Chromatography with Pulse Amperometric Detection (HPAED-PAD) system was employed (Dionex ICS 5000+, Thermo Scientific Inc., USA). The system was equipped with an AS-AP autosampler, an ICS 5000+SP pump and an ICS 5000+DC column oven. An ICS 5000+ED pulsed amperometric detector, with an Au working electrode and an Ag/AgCl reference electrode was used. A CarboPac PA-1 anion exchange column and a CarboPac PA-1 guard column were used and kept at 25 ºC. Elution was performed in isocratic mode with sodium hydroxide (100 mM) for 15 min, followed by a washing step for 5 min with sodium hydroxide (100 mM) in sodium acetate (500 mM). The column was then reconditioned for 5 min with sodium hydroxide (100 mM) before next injection. Flow rate was set at 1 mL/min and an injection volume of 20 μL was employed. All samples were analyzed in duplicate.

2.3. Raman spectroscopy

A RamanRXN2^{TM} Hybrid system (Kaiser Optical Systems, Inc., Ann Arbor, MI, USA) was used to collect the Raman spectra. This instrument was equipped with a wide area non-contact PhAT-probe. A 400 mW laser with a 785 nm excitation wavelength, and a circular spot size of D = 6 mm at a 25 cm working distance was used. Each spectrum was an average of 4x20 sec accumulations, measured in triplicate, giving a total acquisition time of 320 seconds for each sample. The average of the three spectra were taken after fluorescence background correction. The measured spectral range was 200 – 1890 cm^{-1}. All samples were measured during four days in a random sequence to avoid potential systematic variations between days or varieties.

To account for possible heterogeneity of samples, apples were spinned around their own axis during spectral collection. Each sample was first measured with skin. The apples were then peeled with a vegetable peeler and measured again. Finally, juice from each apple was obtained with a juice maker (Philips HR1866/00). The peduncle was removed and the remaining of peeled apple was juiced. The juices were frozen after measuring SSC for further analysis with a different Raman probe. The time for the entire procedure was less than 20 minutes per apple, avoiding oxidation of samples with air.

All juice samples were thawed and measured with a Raman immersion ballprobe (Matrix Solutions, Bothell, WA) suitable for liquids. The ballprobe was 20 cm long and 12.5 mm o.d, incorporating a spherical lens. The instrumental settings were the same as those used for solid samples, again performed in triplicates.

2.4. Depth of Raman measurement

To investigate the sampling depth with Raman in intact apples we performed one simple experiment. A 25 mm thick slice of apple was placed upon a slice of carrot. The skin side of the apple was facing the Raman probe (Figure 1). The apple slice was gradually sliced thinner and thinner from the underside, and for every thickness a Raman spectrum was recorded. The thinnest slice was 2 mm thick. The experiment was done for two apple slices, one without skin and one with red skin. The appearance of the beta-carotene peaks at the different sample thicknesses would give an indication of the sampling depth. Multivariate curve resolution (MCR) was used to extract the pure carrot and apple signals from the spectra (Tauler, 1995), making it possible to estimate the relative contributions from carrot and apple as function of apple slice thickness. MCR was performed in Matlab version R2007b by the PLS_Toolbox (Eigenvector Research Inc., Manson, WA, USA).

2.5. Multivariate data analysis

The fluorescence background in the raw Raman spectra was removed by subtracting a polynomial fitted to the baseline (Lieber and Mahadevan-Jansen, 2003). The procedure was applied to the range 300 - 1500 cm^{-1} because the main information from sugars is in this range. A polynomial degree of 6 was used. The correction was performed using in-house Matlab scripts (R2007b, The MathWorks, Inc., Natick, MA, USA).

Principal component analysis (PCA) (Wold et al., 1987) was applied to explore spectral variation between apple varieties. PCA was performed using The Unscrambler version 6.11 (CAMO Software AS, Oslo, Norway). Partial least-squares regression (PLSR) (Martens and Næs, 1989) was used to obtain calibration models between Raman spectra and the quality features. Full cross-validation and segmented cross-validation (leaving out one apple variety at the time) were used to determine the number of components to use in the calibrations, and to evaluate the performance of the models. Multivariate calibration was performed using The Unscrambler version 6.11 (CAMO Software AS, Oslo, Norway).

3. Results and discussion

3.1. Spectral information

Baseline corrected Raman spectra of apples with and without skin, as well as for apple juice, are presented in Figure 2 (raw spectra are shown in Figure S1). The spectra clearly reveal that Raman spectra of apples are rich in bands and thus chemical information on apple composition. Tentative band assignments are provided in Table 1, and as seen from the list, most bands can be attributed to the carbohydrates sucrose, fructose and glucose (Ilaslan et al., 2015; Özbalci et al., 2013). The most intense bands appear at 629 cm^{-1} and 1459 cm^{-1}. Raman spectra of glucose, fructose and sucrose standards collected in water solution are provided in Figure S2. By comparing the spectra, a range of the bands appearing in apple spectra can be identified in the standards: 420 cm^{-1}

(fructose or glucose); 629 cm^{-1} (fructose), 1084 cm^{-1} (fructose), 1124 cm^{-1} (glucose), 1264 cm^{-1} (fructose) and 1459 cm^{-1} (fructose, sucrose or glucose).

Figure 2 reveals notable similarity between apple juice spectra and spectra of apples without skin. More surprising, taking into account the colorful skin, Raman spectra of apples with and without skin are also very similar. This similarity could be related to the fact that apple skin is rather thin and that we were probing considerably deeper into the apple. The few additional bands found in the spectra of apples with skin is most likely related to skin pigmentation, such as chlorophyll (i.e. the Raman bands found at 746 cm^{-1} and 1327 cm^{-1}) (Jehlička et al., 2014). All spectra in Figure 2 are colored according to SSC (%) values. By visual inspection, a clear trend in the spectra is observed in some regions around 629, 854, 1084, 1124, 1264 and 1459 cm^{-1}. These bands are more intense in samples of high SSC. The trend is more apparent for apples without skin and juices compared with spectra from samples with skin and thus gives initial indications on the quantitative features of the spectra.

To study potential spectral variation among apple varieties, detect potential outliers and systematic artifacts in the samples, PCA was applied. For apples with skin, the second and fourth principal components (PC2 and PC4)), explaining 23 % and 4 % of the variance, respectively, showed a quite clear clustering of samples according to varieties (Figure 3A). Loadings for PC2 (Figure 3B) show that the main variables affecting the separation of varieties were 628, 835, 1083 and 1458 cm^{-1}, representing bands from sucrose and fructose. Scores values for PC2 were generally higher for varieties 2, 3, 5 and 6, which indicates that the concentrations of these compounds tend to be higher in these varieties. This is in accordance with measured sucrose (Figure 5). For PC4, the variables resulting in clustering were 420, 628, 745 and 1326 cm^{-1}. Positive loadings were related with glucose and fructose and negative loadings were related with chlorophyll, showing higher intensity peaks in variety 1, 3 and 5 for these variables.

In the case of apples without skin, PC2 and PC3, explaining 22 and 7 % of variance, respectively, showed some clustering (Figure 3C). Variety 5 was the most clearly clustered group. For PC3, the main variables highlighted were 628, 834, 1124 and 1456 cm^{-1}. Positive loadings (1124 cm^{-1})

were related with glucose, which was very low for variety 5 (Figure 5C). Negative loadings were related with sucrose and fructose, and the concentration of sucrose was high in variety 5. Thus, even though apple skin clearly introduces additional chemical information in the spectra, clear chemical features from apple tissue is seen in both sampling approaches.

3.2. Depth of Raman measurement

A simple experiment was performed to investigate Raman sampling depth in intact apples using a thick slice of apple on top of a slice of carrot. The carrot exhibits strong Raman scattering at 1007 cm^{-1} and 1156 cm^{-1} due to beta-carotene. Figure 4A shows Raman spectra from the apple slices of varying thickness upon the carrot sample. The intensity of the beta-carotene bands increased when the thickness of the apple slices decreased. Based on MCR it was possible to separate the signals from carrot and apple, and the estimated pure spectra are shown in Figure 4B. The corresponding estimated concentrations of carrot and apple for each apple slice thickness are plotted in Figure 4C and 4D. The estimated concentrations were normalized with respect to the signals obtained from pure carrot and apple, respectively, and are therefore estimates of how large shares of the signal that originated from carrot or apple. For an apple slice of 2 mm without skin (Figure 4C) about 55 % of the signal came from the carrot, and for a slice of 5 mm as much as 27 % of the signal still came from carrot. At 8 mm thickness the contribution from carrot was approaching zero. For apple with skin the signal contribution from deeper regions was smaller, about 30 % at 2 mm and 12 % at 5 mm thickness. It was concluded that the current setup was sufficient to probe 7-8 mm into the apple and that the skin reduced the signal from deeper regions. Clearly, most of the Raman signal came from the sample volume close to the apple surface (0-4 mm), but it is interesting that signals are captured from depths down to 8 mm. Similar studies with NIR spectroscopy on apples indicate a sampling depth of only about 4 mm in the 700–900 nm range (Lammertyn et al., 2000), but sampling depth will always depend on the optical setup.

3.3. Quantification of SSC and sugars

The bar charts of Figure 5 show the variation of all the analyzed reference parameters, grouped by variety. For SSC there are similar ranges (minimum and maximum values) across all varieties (Figure 5A). Samples from variety 1 (Granny Smith) and variety 4 (Golden Delicious) had lower total content of sugars than the other four varieties (Figure 5B). Larger span of variation (both between varieties and within each variety) is seen for glucose (Figure 5C) and sucrose (Figure 5E) compared to fructose (Figure 5D). Mean values of fructose for each variety were compared, and statistically differences were found between varieties 6 and 1 and varieties 6 and 5. The correlations found between different reference parameters in the samples were calculated and are provided in Figure S3A. As expected, there was a high correlation between SSC (%) and total sugars. In addition, there were high and positive correlations between sucrose, SSC and total sugars. A strong negative correlation was found between sucrose and glucose. Fructose did not present high correlations towards any other parameter. In general, these correlations are important to take into account when interpreting the calibration models obtained.

Baseline corrected Raman spectra (300 – 1500 cm^{-1}) were used to obtain the calibration models for all chemical reference parameters (Table 2). The optimal number of components were chosen based on the explained variance for each component as well as the regression coefficients, making sure regression coefficients were consisting of distinct spectral features and not only noise. For SCC, the results were good compared to reported studies based on NIRS (Fan et al., 2020; Lan et al., 2020; Li et al., 2018). In general, results based on apples without skin were better than apples with skin. This result could be expected since having to penetrate the skin adds complexity to the spectroscopic measurements. Moreover, reference measurements were obtained from the peeled apples, so a better match could be expected. However, results for the measurements on apples with skin are still acceptable. Regression coefficients for all calibration models for apples without skin are provided in Figure 6. For the SSC regression coefficients (Figure 6A), the main variables affecting the models were found at 834, 1070, 1130 and 1460 cm^{-1}. These variables have been attributed to sucrose in solution (Figure S2C). This result is in accordance with the correlation

found between SSC and sucrose content (Figure S3). Overall, the regression coefficients for total sugars emphasized similar chemical bands as those for SSC.

For glucose and sucrose, good calibration models were obtained, both on apples with and without skin. The regression coefficients for glucose and sucrose were dominated by the same Raman bands, but inversely correlated. This could be expected since the reference values were negatively correlated (Figure S3A). The correlations between the predicted values from these calibration models are shown in supplementary Figure S3B and S3C. Since these correlation coefficients were similar to those obtained for the reference values, it is most likely possible to predict the individual content of sugars independently of the variation of other sugars or total sugars. The poorest regression results were obtained for fructose for all sample types. However, note that the regression coefficients obtained (Figure 6D) (including the following Raman shifts: 423, 523, 629, 1268 and 1460 cm^{-1}) closely resembles the Raman spectrum of aqueous fructose (Figure S2B and Table 1). This means that the model is based on chemical information from fructose. One explanation for poor accuracy is the narrow variation range of fructose, as seen in Figure 5D.

Calibration models for juice were included as benchmarks for the other sampling approaches, since juice samples are more homogeneous without the complex sample matrix of intact apples. Surprisingly, for SCC and total sugars, regression results were better for apples without skin than for juice samples. For single sugars, the regression results obtained on apples without skin were very similar to those of juice. It is difficult to point on one single explanation for these results. For bulk parameters like SCC and total sugars it could be hypothesized that apple matrix bands not directly related to sugars are used indirectly to improve modelling of bulk parameters in the peeled apples. Such matrix bands are obviously not present in juice spectra. Regardless, the results clearly suggest that apple measurements perform as well as juice measurements, which is encouraging for future development of this application.

In this study, all Raman spectra were pre-processed using a standard baseline correction. Additional tests employing a normalization routine (extended multiplicative scattering correction) led to less accurate calibration models (data not shown). Normalization could remove relevant

chemical variation in the Raman spectra. The exploration of pre-processing steps, including baseline correction and normalization, will be an essential part of future development of this approach. Moreover, in order to evaluate the robustness of the Raman measurements, regression models were validated by leaving out one apple *variety* at a time (i.e. 17 % of the samples were left out each time). As provided in Table S1, these results were mainly the same as for full cross-validation. Since robustness across varieties is a major challenge when using NIR spectroscopy, this suggests that Raman could be a beneficial alternative. However, more data is needed to explore this possibility.

To validate current results, sample sets and variation ranges should be extended with new varieties. As only ripe apples with very low starch contents were used, the inclusion of apples from different stages of ripening would also be very interesting. Starch exhibits distinct Raman bands that certainly will affect the overall Raman fingerprints. Another interesting aspect is looking into alternative Raman sampling possibilities. SORS could potentially provide deeper optical sampling than the wide area Raman probe used in the present study, and this might improve current results. SORS is expected to be particularly beneficial in measurements of intact apples, since the SORS approach would enable efficient penetration and suppression of signals from the skin layer.

Compared to NIRS, Raman systems are generally limited by weaker signals. Prolonged exposure times is a common way of compensating for this. The exposure times used in the current study (i.e. 320 seconds) were not optimized with respect to speed, but an achievable aim should be to reduce exposure times down to 2-5 seconds. Furthermore, Raman measurements are very sensitive to ambient light. In this study the measurements were done in a dark room with negligible ambient light, while in field or in processes this has to be solved with proper shielding. In addition, Raman systems tend to be more expensive than NIR systems. The development of Raman technology is currently happening at a steady pace, and it is likely that more affordable systems with improved sampling opportunities and signal efficiency will be available in the near future.

4. Conclusions

This study illustrates the feasibility of using Raman spectroscopy for quantification of SSC and individual sugars (glucose, fructose and sucrose) in apples with and without skin. By using a wide area Raman probe, it is possible to measure at least 8 mm into an apple, through the skin. Calibration models for SSC provided an accuracy comparable with what is achievable with NIRS. In addition, good calibration models were obtained for glucose and sucrose. Poorest models were obtained for fructose. This could be related to the poor variation range of this component in the current sample set. Extending sample sets with new varieties at different stages of ripeness is needed to further validate the feasibility of Raman spectroscopy for use in apple quality evaluation.

Acknowledgements

Hanne Zobel is thanked for practical advices during HPAED-PAD and Karen Wahlstrøm Sanden for skilled technical assistance. The work was funded by the Norwegian Agricultural Food Research Foundation through the projects Precision Food Production (NRC project number 314111) and SusHealth (NRC project number 314599). Olga Monago Maraña thanks to the Fundación Ramón Areces for a postdoctoral fellowship for studies abroad in the field of Life and Matter Sciences (XXXI edition of grants, 2019/2020) to support her postdoctoral studies at Nofima, Ås, Norway.

References

Afseth, N.K., Bloomfield, M., Wold, J.P., Matousek, P., 2014. A novel approach for subsurface through-skin analysis of salmon using spatially offset raman spectroscopy (sors). Appl. Spectrosc. 68, 255–262. https://doi.org/10.1366/13-07215

Cael, J.J., Koenig, J.L., Blackwell, J., 1974. Infrared and raman spectroscopy of carbohydrates. Carbohydr. Res. 32, 79–91. https://doi.org/10.1016/s0008-6215(00)82465-9

Delfino, I., Camerlingo, C., Portaccio, M., Ventura, B. Della, Mita, L., Mita, D.G., Lepore, M., 2011. Visible micro-Raman spectroscopy for determining glucose content in beverage industry. Food Chem. 127, 735–742. https://doi.org/10.1016/j.foodchem.2011.01.007

Esmonde-White, K.A., Cuellar, M., Uerpmann, C., Lenain, B., Lewis, I.R., 2017. Raman spectroscopy as a process analytical technology for pharmaceutical manufacturing and bioprocessing. Anal. Bioanal. Chem. 409, 637–649. https://doi.org/10.1007/s00216-016-9824-1

Fan, S., Wang, Q., Tian, X., Yang, G., Xia, Y., Li, J., Huang, W., 2020. Non-destructive evaluation of soluble solids content of apples using a developed portable Vis/NIR device. Biosyst. Eng. 193, 138–148. https://doi.org/10.1016/j.biosystemseng.2020.02.017

Guan, Y., Peace, C., Rudell, D., Verma, S., Evans, K., 2015. QTLs detected for individual sugars and soluble solids content in apple. Mol. Breed. 35, 1–13. https://doi.org/10.1007/s11032-015-0334-1

Harker, F.R., Gunson, F.A., Jaeger, S.R., 2003. The case for fruit quality: An interpretive review of consumer attitudes, and preferences for apples. Postharvest Biol. Technol. 28, 333–347.

Helgerud, T., Knutsen, S.H., Afseth, N.K., Stene, K.F., Rukke, E.O., Ballance, S., 2016. Evaluation of Hand-Held Instruments for Representative Determination of Glucose in Potatoes. Potato Res. 59, 99–112. https://doi.org/10.1007/s11540-015-9310-8

Ilaslan, K., Boyaci, I.H., Topcu, A., 2015. Rapid analysis of glucose, fructose and sucrose contents of commercial soft drinks using Raman spectroscopy. Food Control 48, 56–61. https://doi.org/10.1016/j.foodcont.2014.01.001

Janick, J., Cummins, J.N., Brown, S.K., Hemmat, M., 1996. Apples, in: Janick, J., Moore, J.N. (Eds.), Fruit Breeding: Volume I. Tree and Tropical Fruits. Wiley, New Jersey, pp. 1–77.

Jehlička, J., Edwards, H.G.M., Oren, A., 2014. Raman spectroscopy of microbial pigments. Appl. Environ. Microbiol. 80, 3286–3295. https://doi.org/10.1128/AEM.00699-14

Lammertyn, J., Peirs, A., De Baerdemaeker, J., Nicolaï, B., 2000. Light penetration properties of NIR radiation in fruit with respect to non-destructive quality assessment. Postharvest Biol. Technol. 18, 121–132. https://doi.org/10.1016/S0925-5214(99)00071-X

Lan, W., Jaillais, B., Leca, A., Renard, C.M.G.C., Bureau, S., 2020. A new application of NIR spectroscopy to describe and predict purees quality from the non-destructive apple measurements. Food Chem. 310, 125944. https://doi.org/10.1016/j.foodchem.2019.125944

Li, X., Huang, J., Xiong, Y., Zhou, J., Tan, X., Zhang, B., 2018. Determination of soluble solid content in multi-origin 'Fuji' apples by using FT-NIR spectroscopy and an origin discriminant strategy. Comput. Electron. Agric. 155, 23–31. https://doi.org/10.1016/j.compag.2018.10.003

Lieber, C.A., Mahadevan-Jansen, A., 2003. Automated method for subtraction of fluorescence from biological Raman spectra. Appl. Spectrosc. 57, 1363–1367.

López, M.G., García-González, A.S., Franco-Robles, E., 2016. Carbohydrate analysis by NIRS-Chemometrics. Intech 13.

Martens, H., Naes, T., 1989. Multivariate Calibration. Wiley, New York.

Monago-Maraña, O., Wold, J.P., Rødbotten, R., Dankel, K.R., Afseth, N.K., 2021. Raman, near-infrared and fluorescence spectroscopy for determination of collagen content in ground meat and poultry by-products. Lwt 140. https://doi.org/10.1016/j.lwt.2020.110592

Nicolaï, B.M., Beullens, K., Bobelyn, E., Peirs, A., Saeys, W., Theron, K.I., Lammertyn, J., 2007. Nondestructive measurement of fruit and vegetable quality by means of NIR spectroscopy: A review. Postharvest Biol. Technol. 46, 99–118.

Özbalci, B., Boyaci, I.H., Topcu, A., Kadilar, C., Tamer, U., 2013. Rapid analysis of sugars in honey

by processing Raman spectrum using chemometric methods and artificial neural networks. Food Chem. 136, 1444–1452. https://doi.org/10.1016/j.foodchem.2012.09.064

Qin, J., Chao, K., Kim, M.S., 2012. Nondestructive evaluation of internal maturity of tomatoes using spatially offset Raman spectroscopy. Postharvest Biol. Technol. 71, 21–31. https://doi.org/10.1016/j.postharvbio.2012.04.008

Richardson, P.I.C., Muhamadali, H., Ellis, D.I., Goodacre, R., 2019. Rapid quantification of the adulteration of fresh coconut water by dilution and sugars using Raman spectroscopy and chemometrics. Food Chem. 272, 157–164. https://doi.org/10.1016/j.foodchem.2018.08.038

Söderholm, S., Roos, Y.H., Meinander, N., Hotokka, M., 1999. Raman spectra of fructose and glucose in the amorphous and crystalline states. J. Raman Spectrosc. 30, 1009–1018. https://doi.org/10.1002/(sici)1097-4555(199911)30:11<1009::aid-jrs436>3.0.co;2-%23

Tauler, R., 1995. Multivariate curve resolution applied to second order data. Chemom. Intell. Lab. Syst. 30, 133–146. https://doi.org/10.1016/0169-7439(95)00047-X

Wang, Q., Li, Z., Ma, Z., Liang, L., 2014. Real time monitoring of multiple components in wine fermentation using an on-line auto-calibration Raman spectroscopy. Sensors Actuators, B Chem. 202, 426–432. https://doi.org/10.1016/j.snb.2014.05.109

Wold, S., Esbensen, K.I.M., Geladi, P., 1987. Principal Component Analysis. Chemom. Intell. Lab. Syst. 2, 37–52.

Table 1. Tentative assignment of Raman bands found in apple samples.

Wavenumber (this work) (cm^{-1})	**Wavenumber reference (cm^{-1})**	**Vibration**	**Compound assigned**	**Reference**
420	415 419	δ(C2 - C1-O1) δ(C - C-O)	Glucose Fructose	(Ilaslan et al., 2015) (Özbalci et al., 2013)
519	523	Skeletal vibration	Glucose	(Ilaslan et al., 2015)
629	631	δ(C–C–O)	Fructose	(Ilaslan et al., 2015)
802	800	ν(C-C)	Sucrose	(Ilaslan et al., 2015)
854	856	δ(C1 – H1)	β-glucose	(Özbalci et al., 2013)
1084	1082	ν(C-O)	Fructose	(Söderholm et al., 1999)
1124	1127	-	β-glucose	(Cael et al., 1974)
1264	1263 1264	-	β-glucose Fructose	(Cael et al., 1974) (Delfino et al., 2011)
1459	1459 1460	$-CH_2$	Fructose Glucose	(Delfino et al., 2011) (Söderholm et al., 1999)

414

Table 2. Results obtained for the different models.

		Apples with skin	Apples without skin	Juices
SSC	**Comp.**	2	1	4
	RMSECV (%)	0.66	0.46	0.72
	R^2	0.70	0.85	0.63
Total sugars	**Comp.**	2	2	2
	RMSECV (mg/L)	9.7	7.5	9.3
	R^2	0.57	0.74	0.61
Glucose	**Comp.**	6	3	3
	RMSECV (mg/L)	2.8	1.9	2.1
	R^2	0.82	0.91	0.90
Fructose	**Comp.**	3	4	3
	RMSECV (mg/L)	6.2	5.6	6.0
	R^2	0.27	0.40	0.32
Sucrose	**Comp.**	5	3	2
	RMSECV (mg/L)	5.8	3.9	3.6
	R^2	0.89	0.95	0.96

415

Figure captions

Figure 1. Sketch of sampling approach for the depth measurement study.

Figure 2. Baseline-corrected Raman spectra from apples with skin (A), apples without skin (B) and apple juices (C). Spectra are colored according to SSC.

Figure 3. Scores values (A and C) and loadings (B and D) obtained from PCA analysis of apples with skin (A and B) and without skin (C and D).

Figure 4. Baseline-corrected Raman spectra obtained for the different slices of apples without skin (A). Estimated pure spectra obtained by MCR (B). Estimated concentrations by MCR for apple without skin (C) and with skin (D).

Figure 5. Bar charts for the different parameters studied: SSC (A), total sugars (B), glucose (C), fructose (D) and sucrose (E). Light colors represent the minimum values, dark colors represent the maximum values and medium color represents the mean value. The error bars represent the standard deviation in each case.

Figure 6. Regression coefficients for the models obtained for apples without skin: SSC (A), total sugars (B), glucose (C), fructose (D) and sucrose (E).

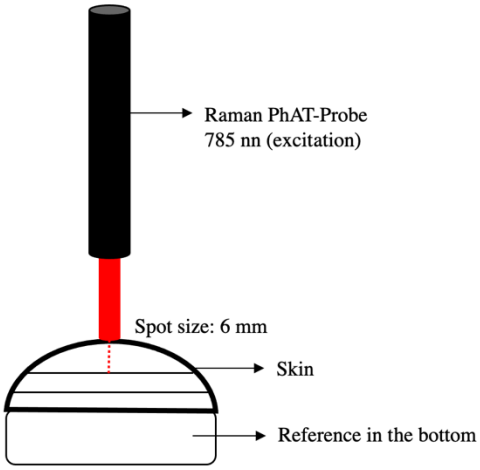

431

432 **Figure 1**

433

434

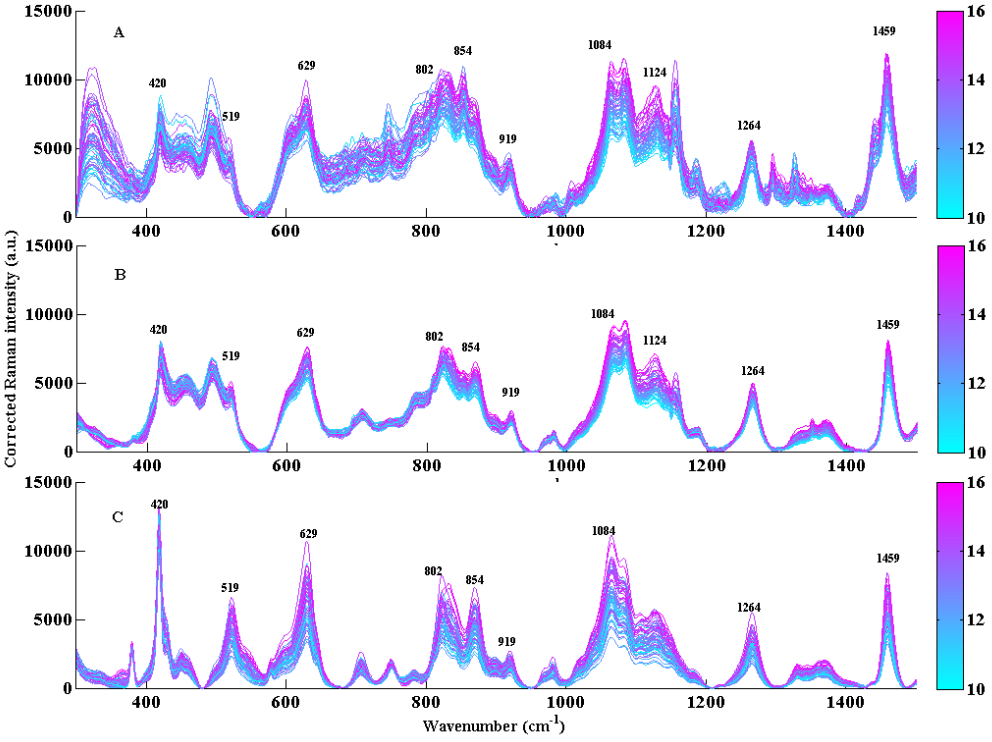

435

436 **Figure 2**

437

438

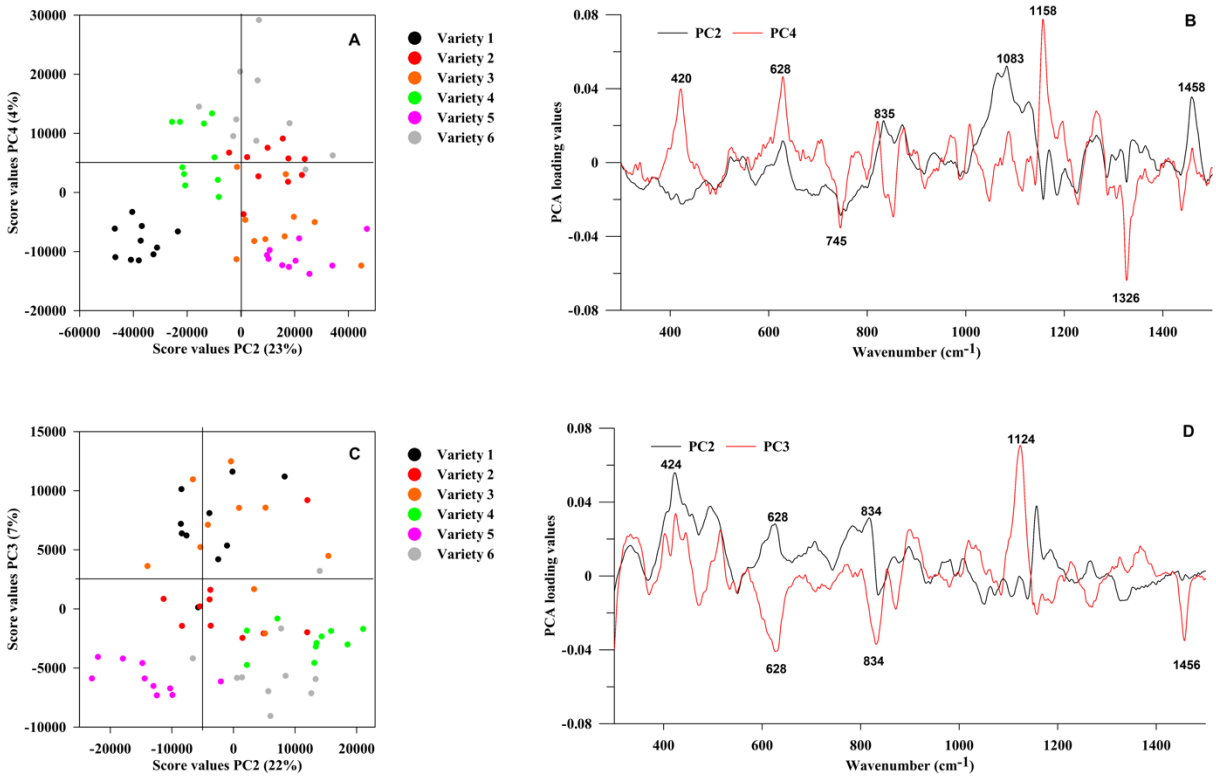

439

440 **Figure 3**

441

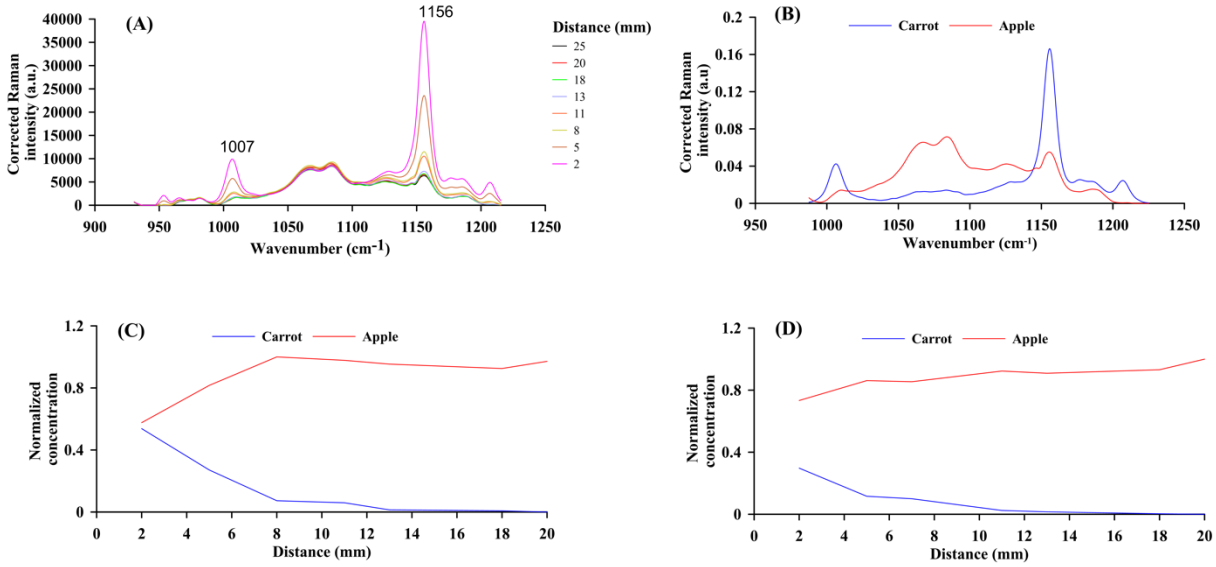

442

443 **Figure 4**

444

445

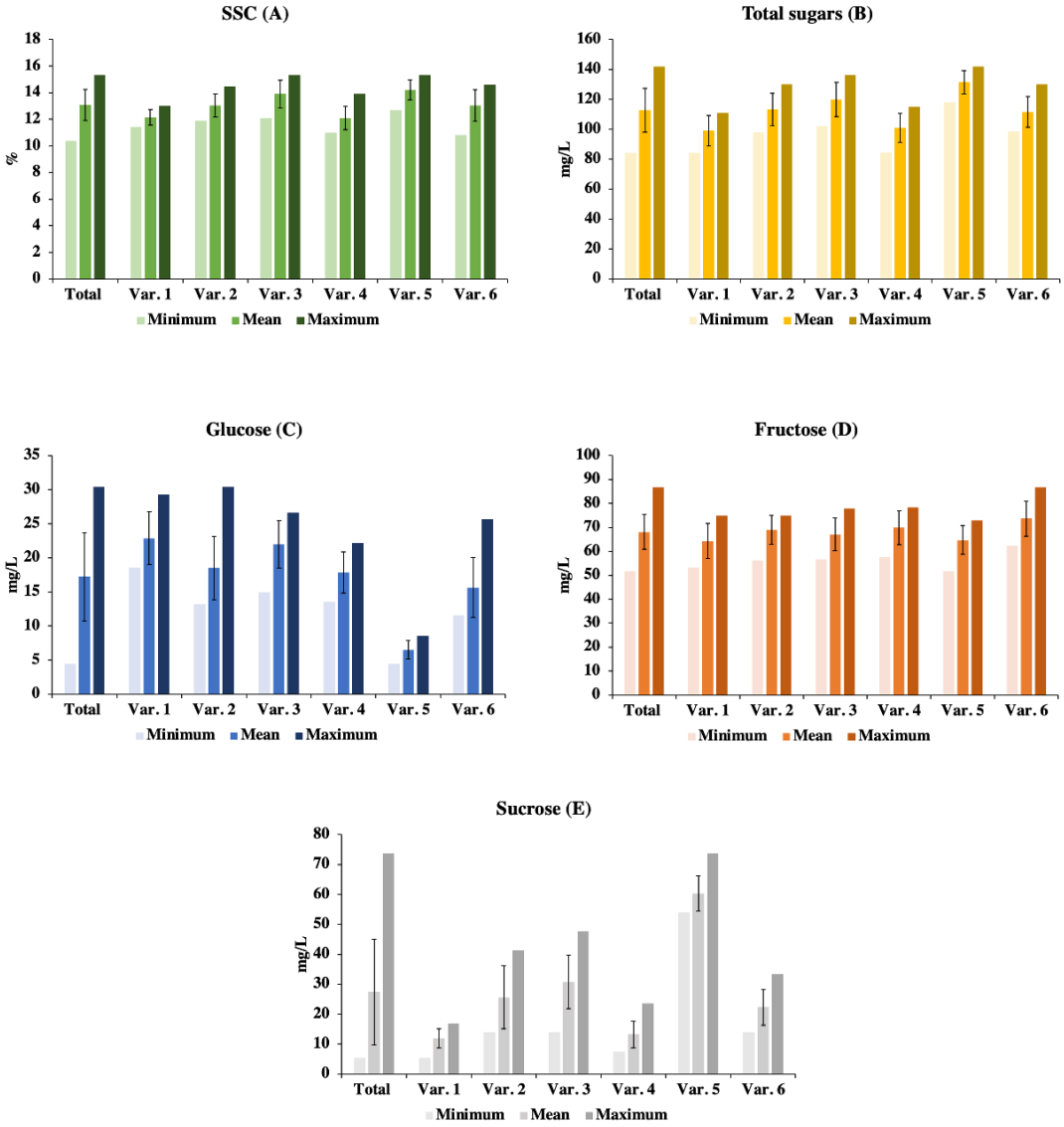
SSC (A)
%
Total
Var. 1
Var. 2
Var. 3
Var. 4
Var. 5
Var. 6
Minimum
Mean
Maximum
Total sugars (B)
mg/L
Glucose (C)
Fructose (D)
Sucrose (E)

Figure 5

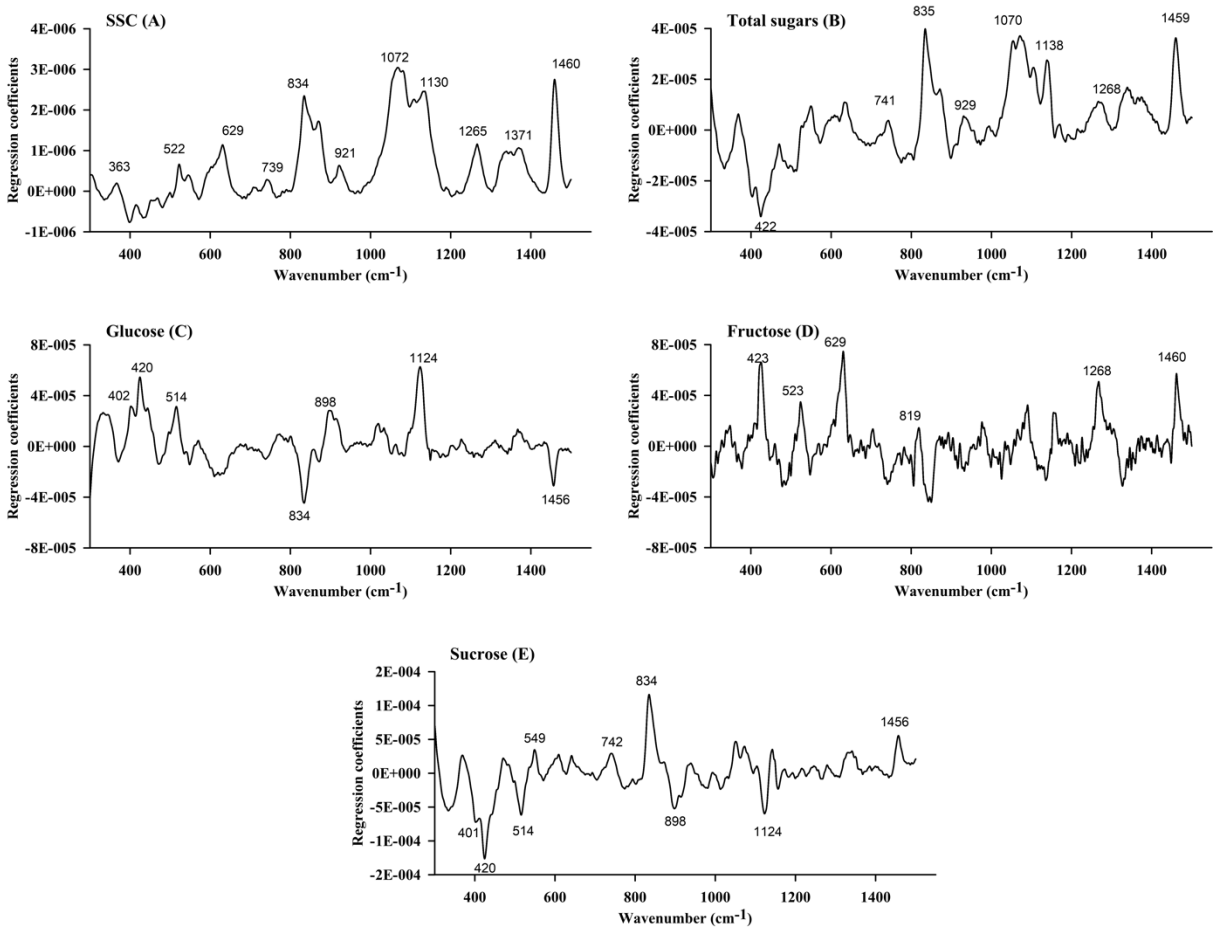

455

456 **Figure 6**